atmosphere

MDPI

Article

Quantitative Mechanisms of the Responses of Abrupt Seasonal Temperature Changes and Warming Hiatuses in China to Their Influencing Factors

Xing Huang, Long Ma *, Tingxi Liu, Bolin Sun, Yang Chen and Zixu Qiao

Department of Resources and Environment, College of Water Conservancy and Civil Engineering College, Inner Mongolia Agricultural University, Hohhot 010018, China; xingxing585@imau.edu.cn (X.H.); txliu@imau.edu.cn (T.L.); 732625667@emails.imau.edu.cn (B.S.); imaucy@emails.imau.edu.cn (Y.C.); linghun@emails.imau.edu.cn (Z.Q.)

* Correspondence: malong@imau.edu.cn; Tel.: +86-1880-471-6707

Abstract: Abrupt temperature changes and warming hiatuses have a great impact on socioeconomic systems; however, their mechanisms remain unclear. In this study, the quantitative mechanisms of the responses of abrupt seasonal temperature changes and warming hiatuses in China to their influencing factors were analysed using the monthly mean temperature (Tav), mean minimum temperature (Tnav), and mean maximum temperature (Txav) from 622 meteorological stations in China covering 1951–2018, the CMIP6 model data, and data at large spatial scales, including Atlantic multidecadal oscillation (AMO) data. The results showed that the contributions of the influencing factors to the abrupt changes in Tav, Tnav, and Txav showed large spatial variability and peaked in the spring and summer and bottomed out in the autumn. The Pacific decadal oscillation (PDO) greatly impacted the abrupt temperature changes in Northeast China and North China at a contribution rate of approximately 12%, strongly influenced the abrupt temperature changes south of the Yangtze River, and markedly influenced the abrupt temperature changes in Northwest China. The AMO had a large impact on temperature in most regions of China in all seasons except for the summer. The MEI mainly affected the abrupt seasonal temperature changes in the region between 25° N and 35° N. The Arctic oscillation (AO) substantially impacted the warming hiatuses in Northeast China in the winter at a contribution rate of approximately 12%. These influencing factors contributed less to warming hiatuses than to abrupt temperature changes. Among the regional influencing factors, AP and WS greatly impacted warming hiatuses, more so than abrupt temperature changes, while relative humidity (RH) and solar radiation (SR) contributed little to warming hiatuses.

Keywords: abrupt temperature change; warming hiatus; influencing factor; quantitative response mechanism; China

check for updates

Citation: Huang, X.; Ma, L.; Liu, T.; Sun, B.; Chen, Y.; Qiao, Z. Quantitative Mechanisms of the Responses of Abrupt Seasonal Temperature Changes and Warming Hiatuses in China to Their Influencing Factors. *Atmosphere* **2023**, *14*, 1090. https://doi.org/10.3390/atmos14071090

Academic Editor: Dae Il Jeong

Received: 12 May 2023
Revised: 12 June 2023
Accepted: 22 June 2023
Published: 29 June 2023

1. Introduction

In long-term climate change research, the mechanisms of abrupt temperature changes and warming hiatuses have attracted much attention. The International Panel on Climate Change assessment report holds that the impact of human activities has caused dramatic changes in temperature, including the warming of the climate caused by the intensification of the greenhouse effect. In contrast, the direct and indirect effects of aerosols offset part of the warming effect. However, since the end of the 20th century, scientists who have been sceptical of drastic climate change have kept questioning the causes of climate warming. Therefore, the causes of drastic climate change, especially the abrupt temperature changes and warming hiatuses, are still a popular research topic worldwide.

First, according to the cumulative curve of precipitation anomalies in different regions of the world, the precipitation in the tropics, North America, South America, Australia, and the east coast of Asia suddenly decreased at the end of the 19th century, and

the phrase "abrupt change" was first used to describe such interannual climate changes (Fu et al., 2015) [1]. Scholars in China and abroad have developed a series of new methods and techniques to identify abrupt changes in temperature, such as moving approximate entropy [2], moving cut data–approximate entropy [3], and detrended fluctuation analysis-based fingerprinting detection [4]. There are two possible causes of transitions or abrupt changes in climate. First, the dynamics of the climate system have not changed during the evolutionary process, and there are only the natural cycles of the cold and warm phases of the climate system, that is, the abrupt phase changes in the system, such as the cycle of spring, summer, autumn, and winter [5]. Second, external forcing or the strengthening (or weakening) of the interaction between the subsystems of the climate system alters the parameters, boundary conditions, or structure of the dynamics of the climate system, thereby causing significant changes in the state variables of the climate system [6]. Many variables in the system that is planet Earth can cause drastic changes in temperature. Generally, influencing factors (or control parameters) of such variables include Arctic sea ice [7], the Greenland and Antarctica ice sheets [8], and the Atlantic meridional overturning current [9]. When these factors reach their turning points, the states of these variables will undergo essential changes, resulting in a drastic change in temperature. Many influencing factors that cause drastic changes in temperature have been investigated. For example, strong volcanic eruptions cause large-scale, drastic climate changes on a variety of time scales through stratospheric volcanic dust veils and volcanic aerosol layers, having an even stronger impact than solar activity and greenhouse gases [10]. The Atlantic sea-surface temperature anomaly associated with the weakening of thermohaline circulation is an important factor causing climate anomalies in Eurasia (including China) [11]. The increase in greenhouse gases significantly raises the mean temperature in summer, resulting in more frequent extreme temperature events [12].

In long-term climate change, another important climate state, the warming hiatus, has a great impact on the entire climate system. During warming hiatuses, tropical wind anomalies have led to severe droughts in western North America [13]. During 1999–2013, the cooling of the Pacific Ocean and warming of the Indian Ocean resulted in profound changes in Asian monsoons [14]. Hiatuses cause frequent severe tropical storms in the coastal areas of East Asia [15]. During warming hiatuses, extremely high-temperature events in summer and extremely low-temperature events in winter occur more frequently in terrestrial areas worldwide [16]. The green-up period is no longer advanced, and the withering period is no longer delayed, indicating that the phenology of vegetation in spring and autumn remains stable [17]. Some researchers believe that these hiatuses are caused by natural external forcing, while others believe that they are triggered by the internal variability of the climate system [18]. The occurrence of hiatuses is partially attributed to La Niña–like cooling in the eastern tropical Pacific Ocean [19]. The weakening of the polar stratospheric vortex leads to hiatuses in Eurasia in winter [20,21].

Past studies on the mechanisms of abrupt temperature changes and warming hiatuses either failed to quantify the responses of abrupt temperature changes and warming hiatuses to their influencing factors by analysing their correlations, or only quantitatively analysed the responses of abrupt temperature changes and warming hiatuses to a single influencing factor by investigating the mechanisms of abrupt temperature changes and warming hiatuses with patterns or models. There are no studies on the quantitative responses of abrupt temperature changes and warming hiatuses to multiple influencing factors. Therefore, this study quantitatively analysed the responses of seasonal abrupt temperature changes and warming hiatuses in China to multiple influencing factors, including large-scale circulation factors, regional influencing factors, and human activity trends, by combining detrending, redundancy analysis, and other methods. The significance of this study is that its results provide a comprehensive basis for climate change research.

To make our research results universal and representative, we selected China as the study area for its wide geologic and climatologic variability. The cooling and warming mechanisms in China are complex and are affected by many factors [22], and the climate

differs significantly between geologic or climate regions. In this study, the quantitative mechanisms of the responses of abrupt seasonal temperature changes and warming hiatuses to their influencing factors were analysed using the monthly data (Tav, Tnav, and Txav) gathered from 622 meteorological stations in China during 1951–2018, the temperature data simulated using different CMIP6 models, and the data of 10 factors that strongly influence temperature changes, including the annual greenhouse gas concentration, CO2, Atlantic multidecadal oscillation (AMO), Pacific decadal oscillation (PDO), the multivariate El Niño southern oscillation index (MEI), and Arctic oscillation (AO).

2. Overview of the Study Area, Data and Methods

2.1. Overview of the Study Area

China is located in the east of Asia, the west coast of the Pacific Ocean (Figure 1), with a land area of about 9.6 × 104 km^2, more than 18,000 km of mainland coastline, more than 14,000 km of island coastline, and more than 4.7 ×104 km^2 of inland and border waters. The climate is complex and varied, ranging from temperate monsoon, tropical monsoon climate, tropical monsoon climate, tropical rainforest, temperate continental climate and highland mountainous, from south to north across the tropical, subtropical, warm temperate, moderate temperate, cold temperate climate zone.

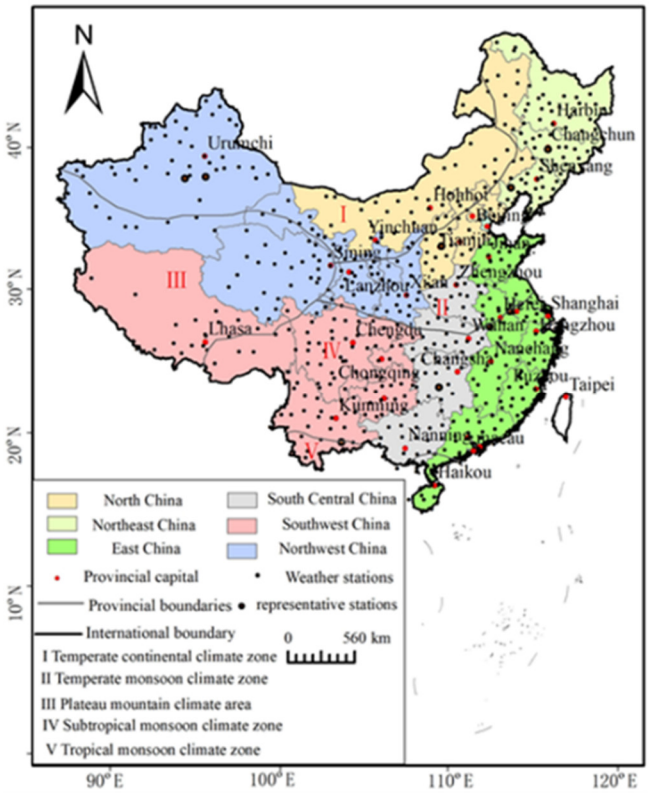

Figure 1. Distribution of stations in the study area.

2.2. Data Sources

The meteorological data used this time are derived from the China Meteorological data network (http://data.cma.cn/) (accessed on 30 June 2022), and 622 meteorological stations distributed in China were selected (Figure 1), which can represent the temperature situation in the study area. In addition, this paper selected 10 influencing factors closely related to temperature change to analyse the attribution of temperature abrupt change and warming hiatus, as follows: AGG, CO2, atmospheric pressure (AP), wind speed (WS) and relative humidity (RH), solar radiation (SR), multivariate El Nino southern oscillation (ENSO) index (MEI), Pacific decadal oscillation (PDO) and Atlantic multidecadal oscillation (AMO). Seven CMIP6 climate system models, namely the Beijing Climate Center Climate System

Model version 2 (BCC-CSM2), the Canadian Earth System Model version 5 (CanESM5), the Centro Euro-Mediterraneo sui Cambiamenti Climatici Earth System Model (ESM) version 2 (CMCC-ESM2), the European Community ESM version 3 (EC-Earth3), the Model for Interdisciplinary Research on Climate version 6 (MIROC6), Additionally, the Max Planck Institute (MPI) ESM version 1.2 in high-and low-resolution configurations (McI-esm1.2-hr and Respectively), were selected. Each model was used to perform two tests, a historical climate simulation test (test 1) and a 21st century climate projection test (test 2), to generate monthly mean surface temperatures, mean minimum surface temperatures, and mean maximum surface temperatures. In test 1, an integral was taken from the mid–late 19st century to December 2005. In test 2, an integral was taken from January 2006 to December 2100 based on the climate data projected for the Shared Socioeconomic Pathway 2–4.5 Scenario. The historical and projected data were combined. The time series Spans from 1951 to 2018 (Table 1).

Table 1. Data and sources.

Data Type	Data Source	Time Series
mean temperature	China Meteorological data network (http://data.cma.cn/) (accessed on 30 June 2022)	1951–2018
mean maximum temperature	China Meteorological data network (http://data.cma.cn/) (accessed on 30 June 2022)	1951–2018
mean minimum temperature	China Meteorological data network (http://data.cma.cn/) (accessed on 30 June 2022)	1951–2018
atmospheric pressure	China Meteorological data network (http://data.cma.cn/) (accessed on 30 June 2022)	1951–2018
Wind speed	China Meteorological data network (http://data.cma.cn/) (accessed on 30 June 2022)	1951–2018
relative humidity	China Meteorological data network (http://data.cma.cn/) (accessed on 30 June 2022)	1951–2018
solar radiation	China Meteorological data network (http://data.cma.cn/) (accessed on 30 June 2022)	1959–2018
CO2/AGG	NOAA Earth System Research Laboratory (Physical Sciences Division)	1979–2018
Pacific Decadal Oscillation	NOAA Earth System Research Laboratory (Physical Sciences Division)	1951–2018
Atlantic multidecadal Oscillation	NOAA Earth System Research Laboratory (Physical Sciences Division)	1951–2018
Multivariate ENSO Index	NOAA Earth System Research Laboratory (Physical Sciences Division)	1951–2018
Arctic oscillation	NOAA Earth System Research Laboratory (Physical Sciences Division)	1951–2018
BCC-CSM2	CMIP6 mode data	1951–2018
CanESM5	CMIP6 mode data	1951–2018
CMCC-ESM2	CMIP6 mode data	1951–2018
EC-Earth3	CMIP6 mode data	1951–2018
MIROC6	CMIP6 mode data	1951–2018
MPI-ESM1-2-HR	CMIP6 mode data	1951–2018
MPI-ESM1-2-LR	CMIP6 mode data	1951–2018

2.3. Data Processing and Utilization Methods

(1) To ensure consistent time series data for the temperature metrics and influencing factors, the missing measurements were filled in through interpolation based on correlation and regression analysis [23].

(2) The Mann–Kendall nonparametric test was used to detect abrupt changes in the temperature metrics and their influencing factors [24].

(3) Based on previous research [25], each year in which a warming hiatus started after an abrupt temperature change (referred to as a warming hiatus year) was identified by analysing the temperature series and its stagewise trend line in combination with the sliding value series for 3 to 5 years and its stagewise trend line. A year was considered a warming hiatus year if it met the following criteria: (1) the climate tendency rate in the year in question reached the relative maximum value after an abrupt temperature change; (2) and the climate tendency rate did not exceed 0.1 °C/10a from the year in question to the end of the series (i.e., 2018) or up to a certain year before the end of the series.

(4) The trends of the time series for the temperature metrics and their influencing factors were analysed based on the climate tendency rate.

(5) The contribution of the natural variability to the temperature metrics was determined using the detrending method [26]. Specifically, the contribution of human activity to the change in each temperature field in China was removed based on the data generated using the CMIP6 models (referred to as CMIP6 model data) to yield the corresponding temperature field for which the natural variability was responsible. The conventional detrending method removes inherent trends in observational data. Because the CMIP6 model data reflected the effects of external forcings, we used the aggregated time series generated using the CMIP6 models to eliminate the effects of human activity on the observed temperature fields in China. The specific procedure was as follows. The abovementioned seven models were ranked based on their temporal and spatial simulation performance. The weight of each model was calculated. A weighted aggregation of the results produced by the models was then produced. Let

$$\overline{T}(n) = \overline{T_F}(n) + \overline{T_I}(n) \tag{1}$$

be the mean observed temperature anomaly field series for China, where F is the external forcings and I is the internal climate variability, that is, natural variability. The mean aggregated model-generated series $\overline{T_m}(n)$ contained the response to the majority of the external forcing fields over the historical period and almost none of the response to the internal climate variability and fit relatively reasonably to the warming trends (correlation coefficient R between ($\overline{T}(n)$ and $\overline{T_m}(n)$ = 0.72). Let $\overline{T_F}(n) = \overline{b_F}\,\overline{T_m}(n)$, where $\overline{b_F}$ is the coefficient of the following regression equation: $\overline{T}(n) = \overline{b_F}\,\overline{T_m}(n) + \&$ (residual term). Then, the nonexternal forcing part can be estimated as follows: $\overline{T_1}(n) = \overline{T}(n) - \overline{b_F}\,\overline{T_m}(n)$. This ensures that $\overline{T_F}(n)$ and $\overline{T_I}(n)$ are uncorrelated (R = 0.03). While $\overline{b_F}\,\overline{T_m}(n)$ contains the changes in the majority of the external forcings in the historical data, $\overline{T_I}(n)$ may still contain some external forcing-related information that is missing in the aggregated model-generated series. Thus, $\overline{T_I}(n)$ is considered the primary part of the natural variability. Based on this principle, the temperature at station i in the nth year, $T(n,i)$, can be expressed as follows:

$$\overline{T}(n,i) = \overline{T_F}(n,i) + \overline{T_I}(n,i) + \&_F(n,i) \tag{2}$$

The temperature change has four components, namely the contribution of the external forcings $\overline{T_F}(n,i)$, the contribution of the natural variability $\overline{T_I}(n,i)$, the contribution of the local response to the external forcings $\&_F(n,i)$, and the contribution of the local response to the natural variability $\&_I(n,i)$. The last two terms have a nonsignificant

impact on the long-term interdecadal temperature change and are thus negligible; therefore, only the impact of the first two terms is considered. Then, we have

$$\overline{T_I}(n,i) = \overline{T}(n,i) - \overline{T_F}(n,i) = \overline{T}(n,i) - \overline{b_F}(i)\overline{T_m}(n) \quad (3)$$

where $\overline{b_F}(i)$ is the regression coefficient obtained from the regression of the observed temperature $\overline{T_I}(n,i)$ upon $\overline{T_m}(n)$. In the above equations, the temperature anomaly field (relative to the period 1951–1990) is used to eliminate the errors in the values simulated using the models for the reference period, with the goal of minimizing the overall error.

(6) The three temperature fields were decomposed via EOF analysis [27]. The principle of EOF analysis is to decompose a meteorological element field into multiple independent linear combinations of time coefficients and spatial vectors, thereby basically reflecting the information contained in the original meteorological element field.

(7) A temperature change is the result of the combined action of multiple factors. Observational information contains both information on the internal natural changes within the climate system and information on the response to natural and anthropogenic external forcing factors. Therefore, producing accurate estimates of the relative contributions of various external forcing factors to climate change is fairly difficult. If (1) the effects of anthropogenic factors are first removed from the observation data based on the CMIP6 model data and (2) the response of the observed temperature fields to various types of natural variability is assumed to be independent and linear, then the following stepwise regression approach can be used to estimate the relative contribution of the natural variability to the abrupt temperature changes and warming hiatuses in China:

$$\mathrm{y} = \mathrm{a}x_1 + bx_2 + cx_3 + \ldots + mx_8 + \varepsilon \quad (4)$$

where y is the detrended observed temperature; x_1, x_2 ... , x_n are the regression coefficients of the influencing factors at the meteorological station (which are estimated based on the annual mean anomaly time series in an order based on the magnitude of the explained variance of each influencing factor at each station for the observed temperature); and ε is the residual term. This approach can ensure that the sum of the contributions of different influencing factors to abrupt temperature changes and warming hiatuses is less than the observed changes.

(8) Linear model-based RDA

In this study, three temperature metrics were treated as response variables, while the selected influencing factors were input as explanatory variables. Principal component analysis—a multivariate statistical analytical method—was used to perform a reduced-dimensional analysis on the influencing factors. In addition, partial RDA (pRDA) was carried out to separate the variances of the influencing factors to quantify the contribution rates (CRs) of different influencing factors for abrupt temperature changes and warming hiatuses (i.e., the proportions of the total contribution of the natural variability to abrupt temperature changes and warming hiatuses for which different influencing factors were responsible).

3. Analysis and Results

3.1. Spatial Distribution of Seasonal Temperature Abrupt Change Years and Warming Hiatus Years Relationships between the Influencing Factors and Tav, Tnav, and Txav in China

Figure 2 shows that although there are deviations between the observed and simulated series of seasonal Tav, Tnav, and Txav in China, their overall fluctuation characteristics are consistent with each other. The simulated series after 2007 has slightly higher temperatures than the observed series. In addition, the observed series are significantly correlated with the series simulated using all models, indicating the excellent performance of these models in simulating the trends of seasonal Tav, Tnav, and Txav in China (i.e., the rising trend of temperature attributed to human activities). The temperature changes attributed to

the seasonal natural variability are obtained by removing from the simulated series the contribution of human activities to the Tav, Tnav, and Txav changes at the 622 stations.

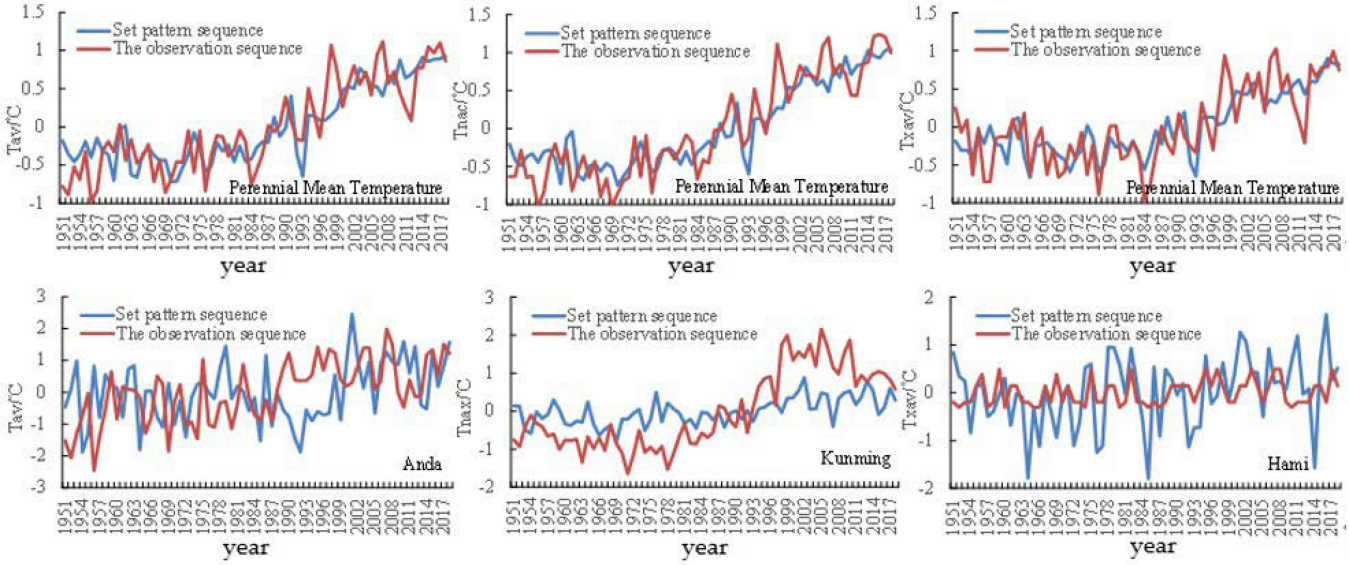

Figure 2. Observed and simulated series of anomalies of Tav, Tnav, and Txav in China.

3.2. Quantitative Response Mechanisms of Abrupt Temperature Changes and Warming Hiatuses

To further illustrate the contribution of the selected influencing factors to the abrupt changes and warming hiatuses in seasonal Tav, Tnav, and Txav, the ensemble empirical mode decomposition (EEMD) method was applied to decompose the observed series of Tav, Tnav, and Txav and the time series of the influencing factors obtained at all 622 stations in China. After decomposition, intrinsic mode functions at different time scales and a residual term were obtained, and the contributions of the influencing factors to each temperature change were quantified using the linear model-based redundancy analysis of the nonlinear trend term. Then, the time periods were classified into the periods before and after the abrupt changes in seasonal temperature and the periods before and after the warming hiatuses at the 622 stations (Figure 3) to quantitatively analyse the contributions of the influencing factors in the periods of abrupt changes and in the periods of warming hiatuses.

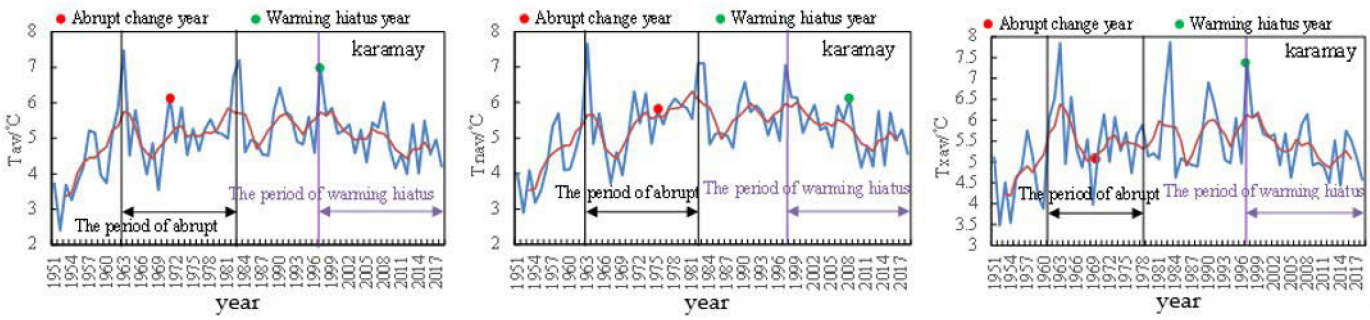

Figure 3. Classification of the periods of abrupt changes and the periods of warming hiatuses at representative stations.

The Tav, Tnav, and Txav at the 622 meteorological stations were computed using the above method. Below, we detail the computation process of a representative station as an example. The selected influencing factors were divided into two categories. The first category was composed of the atmospheric circulation factors, including the PDO, AMO, MEI, and AO. The second category consisted of regional influencing factors, including RH, SR, WS, and AP. Figure 4 shows that the contribution rates of the atmospheric circulation factors were 25.9–48% in the periods of abrupt changes and 19.9–32.8% in the periods of warming

hiatuses, and that the contributions of the regional influencing factors were 11.5–19.7% in the periods of abrupt changes and 13.2–29.7% in the periods of warming hiatuses.

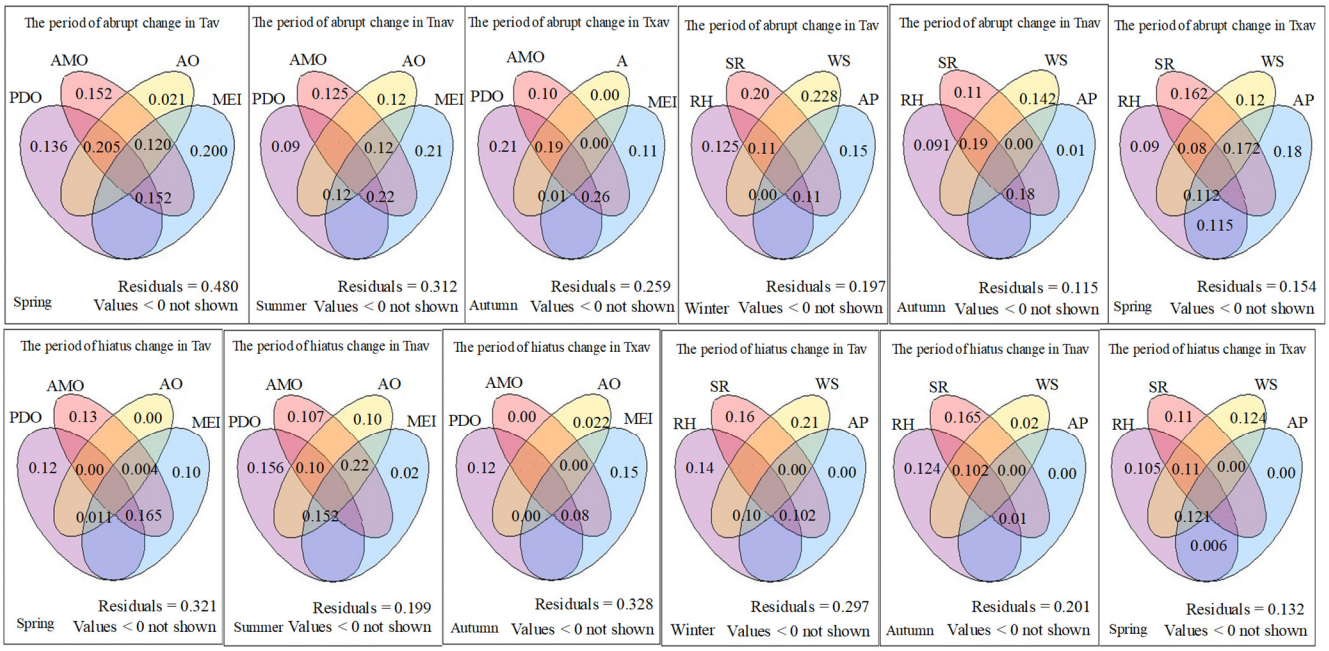

Figure 4. Variance analysis of factors influencing the abrupt temperature changes and warming hiatuses based on partial redundancy analysis.

According to the above computation process, the contributions of each influencing factor to the periods of abrupt changes in seasonal temperature and to the periods of warming hiatuses were interpolated across space. Figure 5 shows that the overall contributions of the PDO to the abrupt temperature changes in different seasons followed the descending order of spring > winter > summer > autumn. The contributions of the PDO to the abrupt changes in Tav, Tnav, and Txav followed the descending order of Tnav > Tav > Txav and were greater in northern China than in southern China, even given the significant seasonal differences. The contributions of the PDO to the abrupt temperature changes in spring were relatively large (approximately 6–8%) in Northeast China and regions north of the Loess Plateau. The regions where the PDO made large contributions to the abrupt changes in Tav and Txav shifted southeastward and northward in the summer compared with in the spring, and the regions where the PDO made large contributions to the abrupt changes in Tnav were concentrated in the regions of Guangdong and Guangxi Provinces characterised by hills. The contributions of the PDO to the abrupt temperature changes in the summer (approximately 2–5%) were generally lower than those in the spring. The PDO contributed less to the abrupt temperature changes in the autumn than those in the spring and summer, as it barely had any effect on over half of the regions of China in the autumn. The contribution rates (approximately 10% to 12%) of the PDO to the abrupt temperature changes in the winter were the largest among all seasons in regions except for the southern Tibetan Plateau and some areas of the Yunnan–Guizhou Plateau.

The contributions of the PDO to the warming hiatuses in the four seasons followed the descending order of winter > spring > summer > autumn, which is similar to the seasonal ranking of the contributions of the PDO to Tav, Tnav, and Txav. The regions where the PDO made large contributions (approximately 9–11%) to the warming hiatuses in spring were concentrated in Northeast China. In contrast, the PDO essentially had no effect on the warming hiatuses in Northwest China. The regions where the PDO made relatively large contributions (approximately 6–7%) to the warming hiatuses of Tav, Tnav, and Txav in the summer were concentrated in the regions north of the Loess Plateau and the plains of the middle and lower reaches of the Yangtze River. PDO contributed to the warming

hiatuses in Northeast China significantly less in the summer than in the spring; however, it contributed less in the autumn among all seasons in all regions except for the central region of the Inner Mongolia Plateau (its contribution rates in this region were approximately 4–7%). The contributions (reaching 15%) of the PDO to the warming hiatuses were greatest in the winter among all seasons.

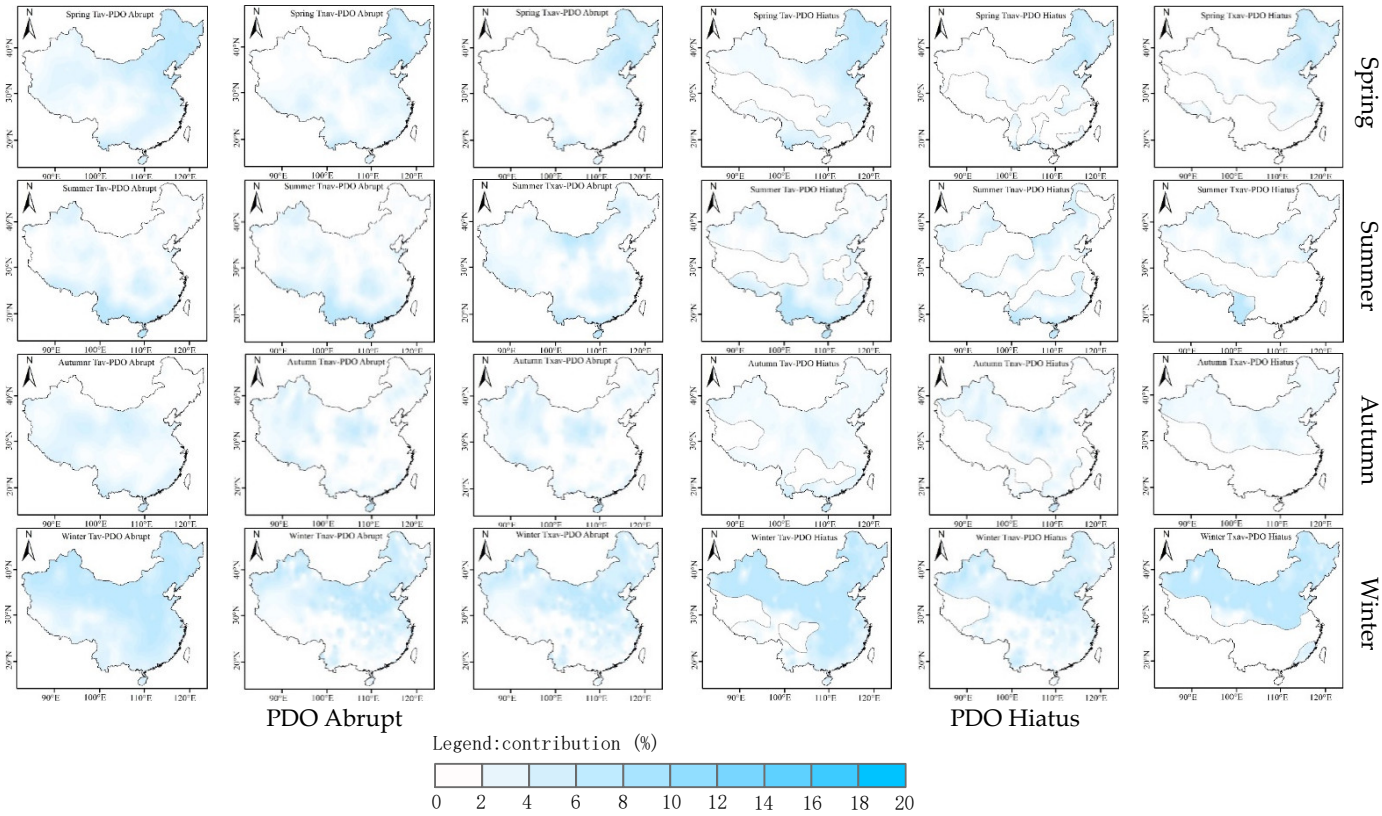

Figure 5. Spatial distribution of the contributions of the PDO to the abrupt seasonal changes and warming hiatuses in Tav, Tnav, and Txav.

Overall, the contributions of the AMO to the abrupt temperature changes in Tav, Tnav, and Txav were greater than those of the PDO. The contributions of AMO to the abrupt changes in Tav, Tnav, and Txav in the different seasons were slightly different in spatial distribution and followed the descending order of autumn > summer > spring > winter (Figure 6). The contribution rates of the AMO to the abrupt changes in Tav, Tnav, and Txav in the spring were close to 0 in Northeast China and the northern part of Northwest China and were larger (approximately 12–15%) in the other regions. The contribution rates of the AMO to the abrupt temperature changes in the summer became low (0.2–0.6%) in the North China Plain and the plains of the middle and lower reaches of the Yangtze River and remained low in the northern part of Northwest China. The contributions of the AMO to the abrupt temperature changes in the autumn (10–12%) had a similar overall spatial distribution but greater values than those in the spring. The contributions of the AMO to the abrupt temperature changes in the winter were small (approximately 1%) in the regions north of 40° N and near the regions of Guangdong and Guangxi characterised by hills, and 8–9% in other regions.

In the spring, the contribution rates (6–7%) of the AMO to the warming hiatuses had a similar spatial distribution but lower values than its contributions to the abrupt temperature changes; however, its overall contributions to warming hiatuses were smaller than its overall contributions to abrupt temperature changes. AMO made large contributions to the warming hiatuses (11–12%) in the regions west of the Inner Mongolia Plateau, the regions west of the Turpan Basin, and the regions from the Tibetan Plateau to the south of

the Yunnan–Guizhou Plateau and smaller ones (<5%) in other regions. In the autumn and winter, the contributions of the AMO to the warming hiatuses had a similar spatial distribution but lower values compared with its contributions to abrupt temperature changes. Therefore, the contributions of AMO to abrupt temperature changes had an essentially similar spatial distribution but greater values than its impact on warming hiatuses.

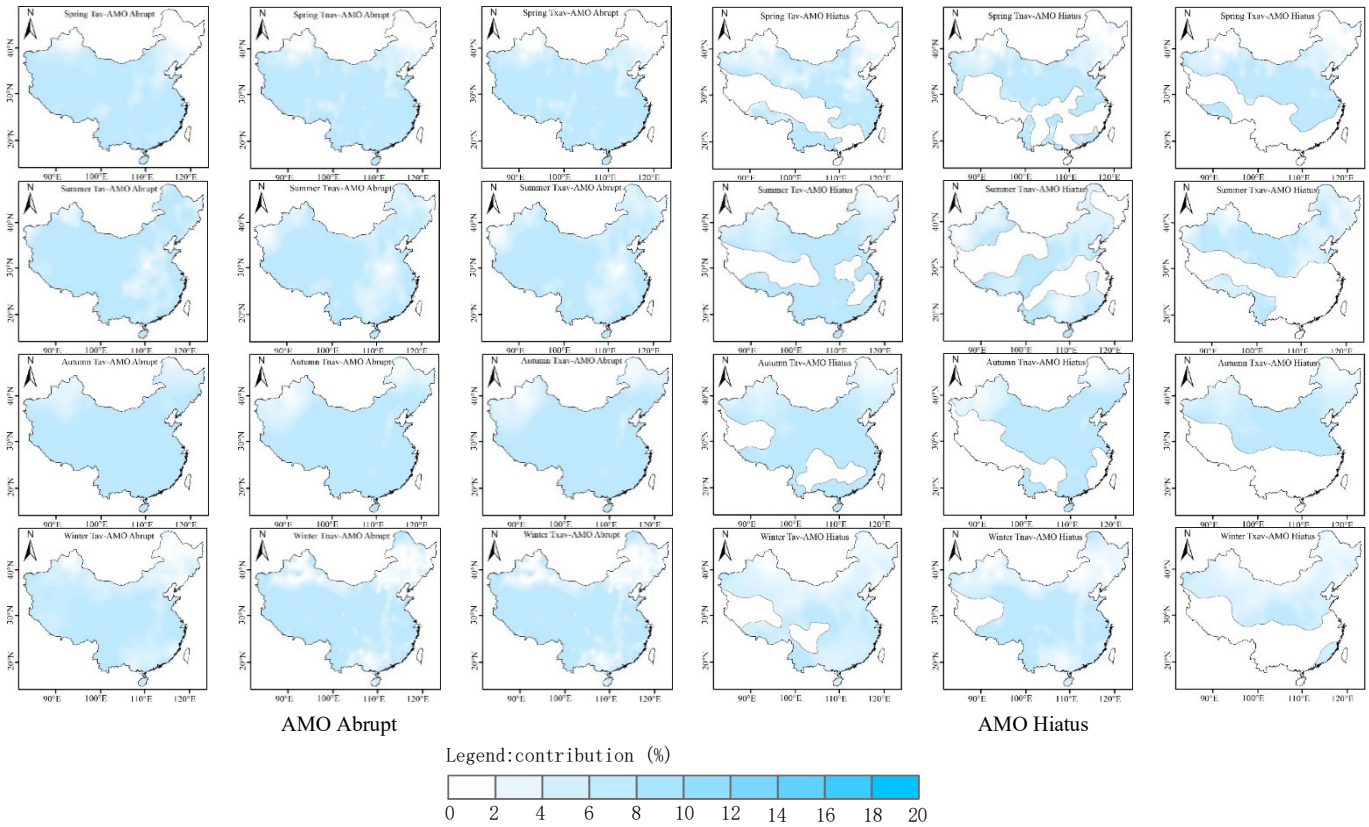

Figure 6. Spatial distributions of the contributions of the AMO to the abrupt changes and warming hiatuses in Tav, Tnav, and Txav.

The contribution rates of the MEI to the abrupt changes in Tav, Tnav, and Txav had essentially similar values but marked seasonal differences in the descending order of winter > spring > autumn > summer. In the spring, MEI made small contributions to the abrupt changes in Tav, Tnav, and Txav in the regions between 25° N and 35° N, but large ones (8–10%) in the regions south of 30° N and north of 35° N. In the summer, the overall contributions of the MEI to the abrupt temperature change were small in all regions other than the southern Yunnan–Guizhou Plateau (its contributions in this region were approximately 3–6%). In the autumn, the MEI made apparent contributions to the abrupt temperature changes in the Loess Plateau and the Inner Mongolia Plateau only (approximately 6% at most), made almost no contributions in Northeast or Northwest China, and made small contributions in the other regions. In the winter, the contribution rates of the MEI to the abrupt temperature changes were 9–13% in all regions other than the southern part of the Tibetan Plateau. The contributions of the MEI to the warming hiatuses were largest in the winter in northern China. In all seasons, the contributions (approximately 10%) of the MEI to the warming hiatuses had a similar spatial distribution but lower values compared with its contributions to abrupt temperature changes (Figure 7).

The contributions of the AO to the abrupt changes in Tav, Tnav, and Txav followed the descending order of Tav > Tnav > Txav. The contributions of the AO to the abrupt temperature changes in different seasons followed the descending order of winter > spring > autumn > summer. The overall contributions of the AO were largest (approximately 12%) in Northeast China. In the spring, the contributions of the AO to

the abrupt temperature changes were larger in Northeast China (6–10%) and the North China Plain and the northern part of Northwest China (7–11%) and smaller in the Tibetan Plateau, the Loess Plateau and most regions in the Zhejiang and Fujian Provinces that are characterised by hills. The overall contributions of the AO to the abrupt temperature changes in summer (<8%) were smaller than that in spring; however, the contributions of the AO to the abrupt temperature changes in the Yunnan–Guizhou Plateau were higher in summer than in spring. In autumn, the AO had a wider impact on but smaller contributions (overall contributions were approximately 3–5%) to the abrupt temperature changes compared with summer. In winter, the AO had the largest contributions to the abrupt temperature changes among all seasons, and it mainly impacted the abrupt temperature changes in Northeast China (a maximum contribution of 13%) and barely impacted the abrupt temperature changes in the regions south of the Loess Plateau. In the spring, the AO had a wider and more intense impact on warming hiatuses (contributions of 10–14%) than on abrupt temperature changes. In the summer, the contributions of the AO to the warming hiatuses had a similar spatial distribution compared with its contributions to abrupt temperature changes. In the autumn, the contributions of the AO to warming hiatuses had a similar spatial distribution but lower values compared with its contributions to abrupt temperature changes. In the winter, the contributions of the AO to warming hiatuses were greater than its contributions to abrupt temperature changes, especially in Northeast China (contributions of approximately 12%). Based on these results, the AO greatly impacted the warming hiatuses in winter but slightly impacted the abrupt temperature changes and the warming hiatuses in summer. The leading factor that caused the abrupt changes was in the mid-high latitude terrestrial regions, and the abrupt changes advanced from north to south; therefore, the abrupt changes occurred the latest in the southern latitude zones (Figure 8).

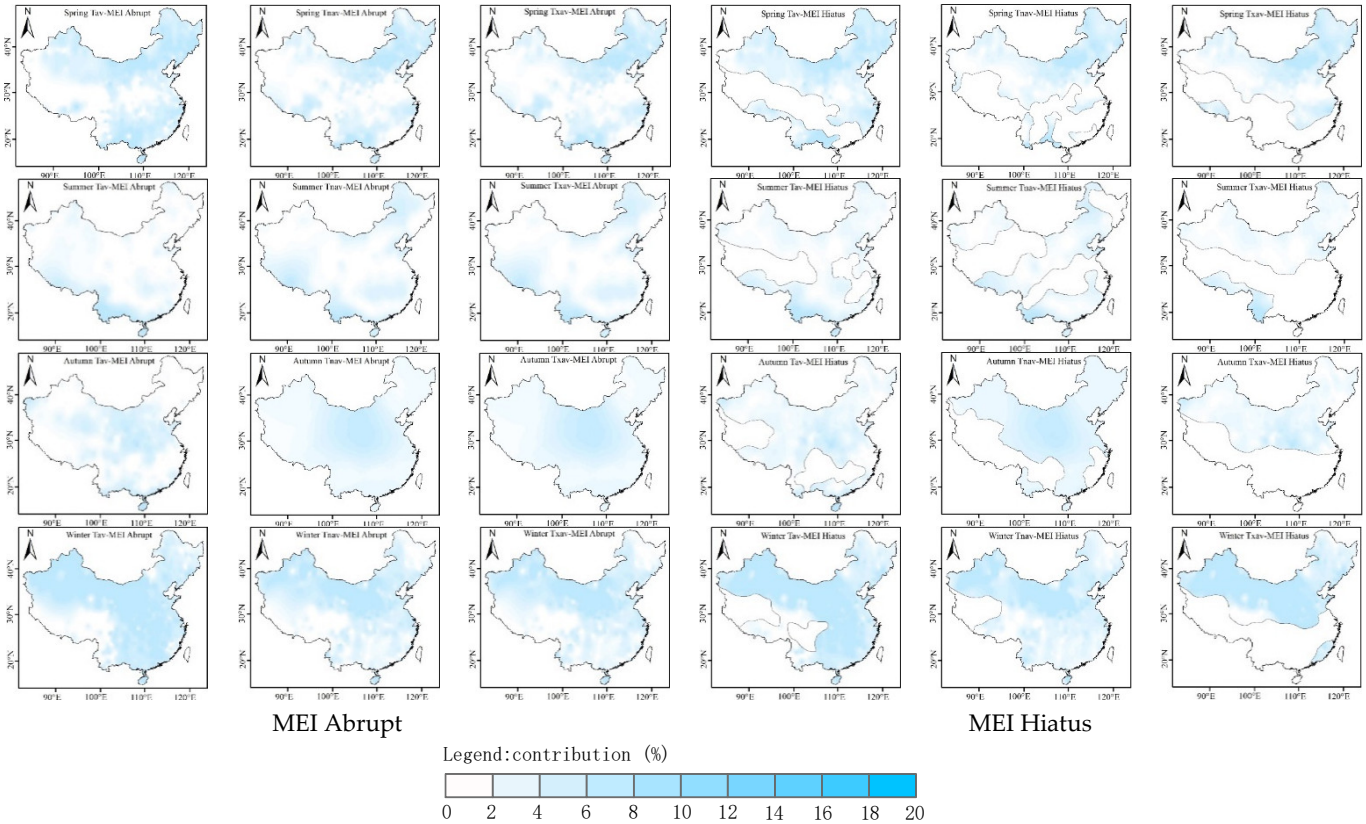

Figure 7. Spatial distributions of the contributions of the MEI to the abrupt changes and warming hiatuses in Tav, Tnav, and Txav.

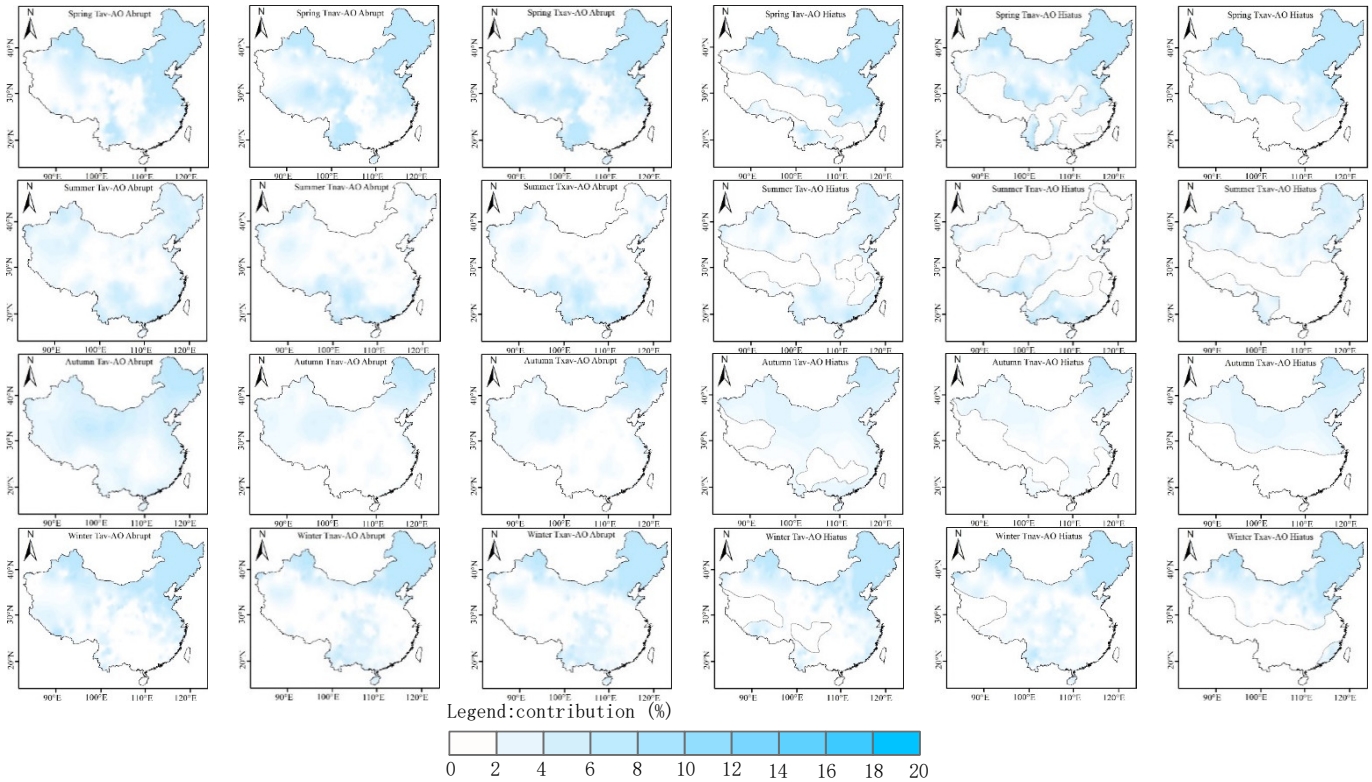

Figure 8. Spatial distributions of the contributions of the AO to the abrupt changes and warming hiatuses in Tav, Tnav, and Txav.

The contributions of RH to the abrupt changes in Tav, Tnav, and Txav followed the descending order of Tav > Tnav > Txav, and the overall effect of RH on the abrupt temperature changes weakened from east to west. The RH weakly impacted the abrupt temperature changes in Tibetan Plateau and mainly affected the regions other than the Tibetan Plateau (contribution of 10–12%). The regions with low contributions of RH to the abrupt temperature changes shifted towards the Yangtze River basin from the spring to the summer. In the summer, the contributions of RH to the abrupt temperature changes were low in the regions between the Yangtze River and the Yellow River but high (7% to 10%) in the other regions. In the autumn, the contributions of RH to the abrupt changes in Tav were higher than its contributions to the abrupt changes in Tnav and Txav (<5%) and were lower in the eastern part of the Tibetan Plateau than in other regions (contributions of 5–7%). In the winter, the contributions of RH to the abrupt changes were low in the Tibetan Plateau and the Yunnan–Guizhou Plateau and 5–7% in other regions. In the spring, RH contributed much to warming hiatuses (3–5%) in the vicinity of the plains of the middle and lower reaches of the Yangtze River. In the summer, the contributions of RH to the warming hiatuses gradually decreased from northeast to northwest. In the autumn, the contributions of RH to the warming hiatuses were high (2–4%) in the Northeast and Northwest China. In the winter, RH contributed less to warming hiatuses (<3%) than in autumn (Figure 9).

The contributions of SR to the abrupt changes in Tav, Tnav, and Txav followed the descending order of Txav > Tnav > Tav in spring and the descending order of Tnav > Tav > Txav in other seasons (Figure 10). Unlike other influencing factors, SR had relatively large spatial variability in its contributions to the abrupt changes in Tav, Tnav, and Txav in all seasons. In the spring, the contributions of SR to the abrupt changes in Tav were largest (approximately 5–7%) in the northern part of Northeast China, the Tibetan Plateau, the Yunnan–Guizhou Plateau, and the regions in Guangdong and Guangxi characterised by hills; the contributions of SR to the abrupt changes in Tnav were largest (approximately 5%) in the regions in Zhejiang and Fujian characterised by hills and the Yunnan–Guizhou Plateau; and the contributions of SR to the abrupt changes in Txav were smallest in the Tibetan Plateau. In the summer, the

contributions of SR to the abrupt changes in Tav and Tnav had similar spatial distributions and were largest (approximately 6–9%) on the plains of the middle and lower reaches of the Yangtze River, while its contributions to the abrupt changes in Txav were largest (3–4%) in Northeast China, Northwest China, and the regions south of the middle reaches of the Yangtze River. In the autumn, the contribution rates of SR to the abrupt changes in Tav and Tnav decreased from northwest to southeast and approached 0 in the regions south of the lower reaches of the Yangtze River, and the SR only affected the abrupt changes in Txav in the eastern part of the Inner Mongolia Plateau (with a rate of approximately 3%). In the winter, Tav was basically unaffected by SR in the region south of the middle and lower reaches of the Yangtze River, while Tnav was less affected by SR overall, and SR made large contributions to the abrupt changes in Txav (6–7%) on the Northeast and North China Plains. The overall contributions of SR to the seasonal warming hiatuses had a similar spatial distribution but smaller values than its contributions to the abrupt temperature changes.

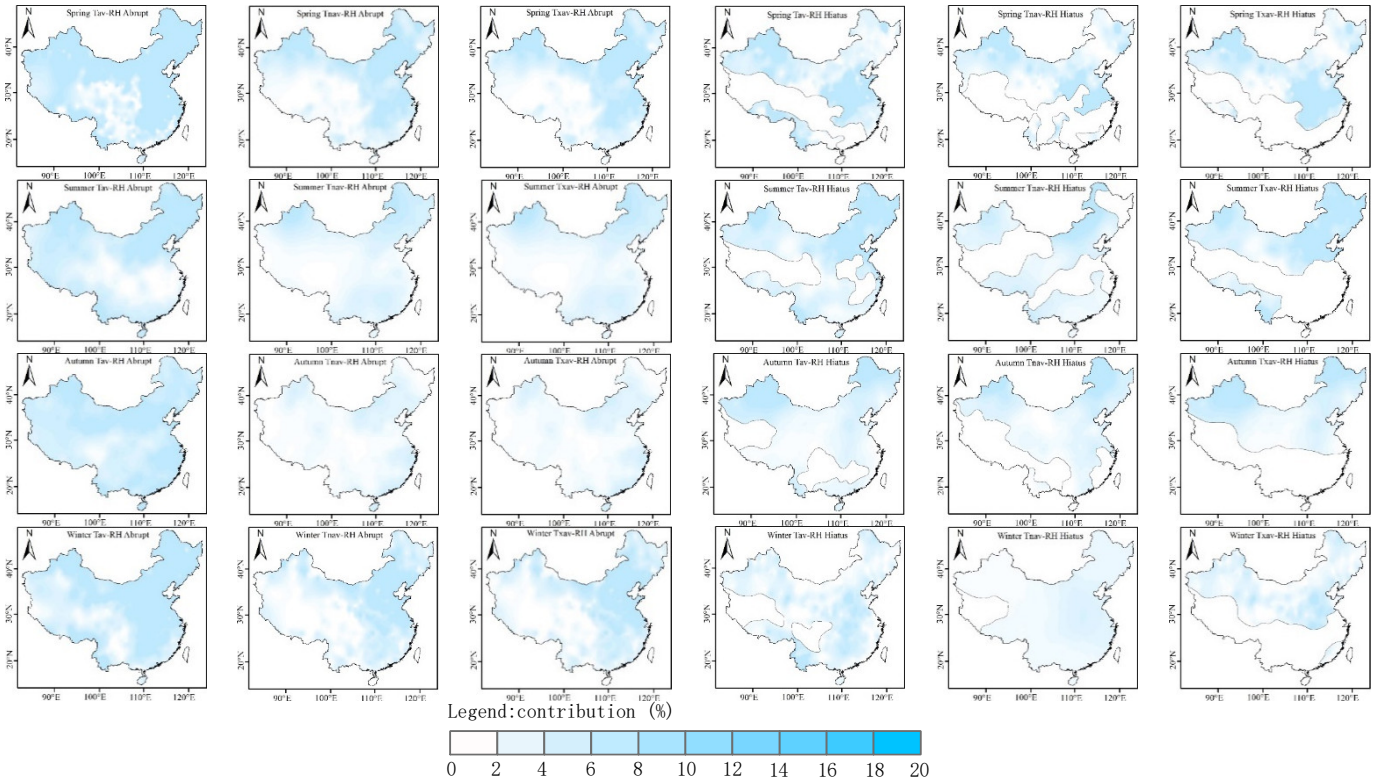

Figure 9. Spatial distribution of the contributions of RH to the abrupt changes and warming hiatuses in Tav, Tnav, and Txav.

WS contributed more than other regional influencing factors to abrupt changes and warming hiatuses in China, and WS impacted the abrupt temperature changes and warming hiatuses in all seasons at similar intensities. In spring, the contributions of WS to the abrupt temperature changes were overall greater in the north than in the south (Figure 11). Its contribution rates were smallest in the regions of Guangdong and Guangxi that are characterised by hills and the Yunnan–Guizhou Plateau and were 8–11% in other regions. In the summer, the contributions of WS to abrupt temperature changes were weak on the plains of the lower reaches of the Yangtze River and 8–10% in other regions. In the autumn, the overall contribution rates (6–9%) of WS to abrupt temperature changes had a similar spatial distribution but lower values compared with those in the summer. In the winter, the contribution rates of WS to abrupt temperature changes were weaker than those in autumn and approached 0 in the regions south of the middle and lower reaches of the Yangtze River and some regions in Northwest China, while they were 8–10% in other regions.

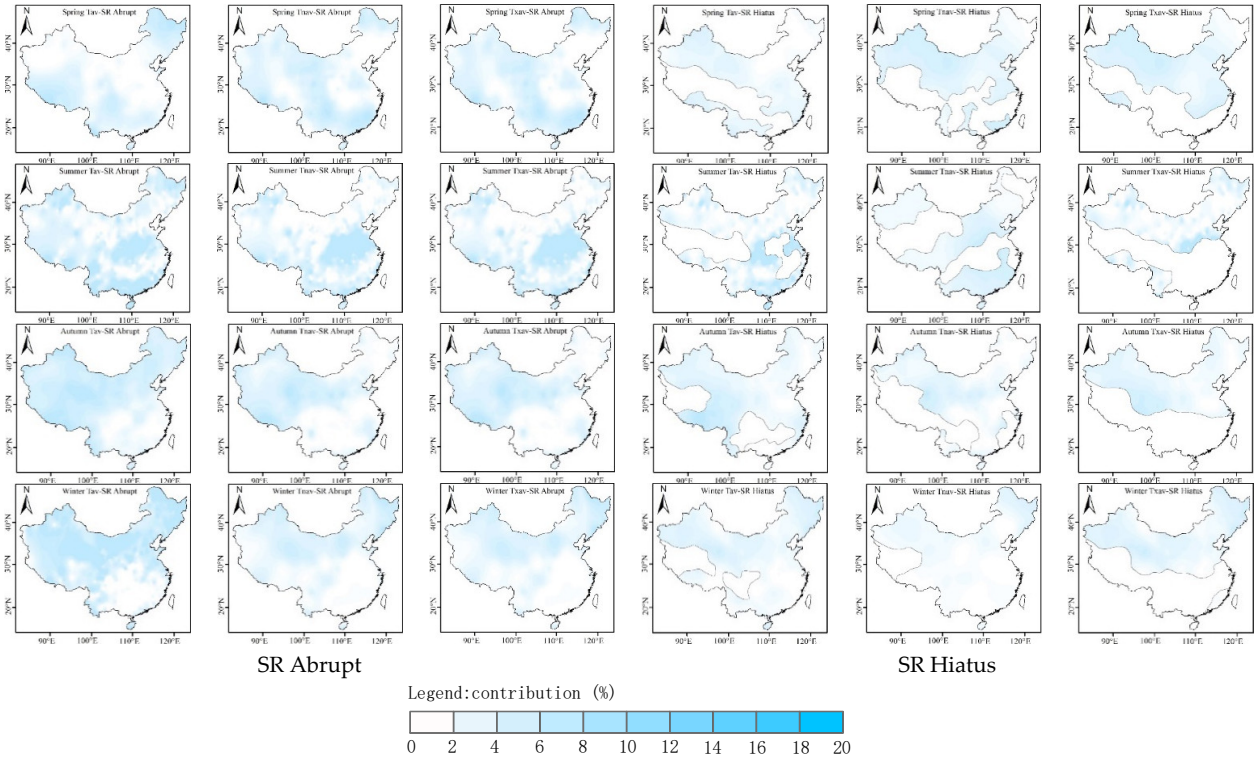

Figure 10. Spatial distributions of the contributions of SR to abrupt changes and warming hiatuses in Tav, Tnav, and Txav.

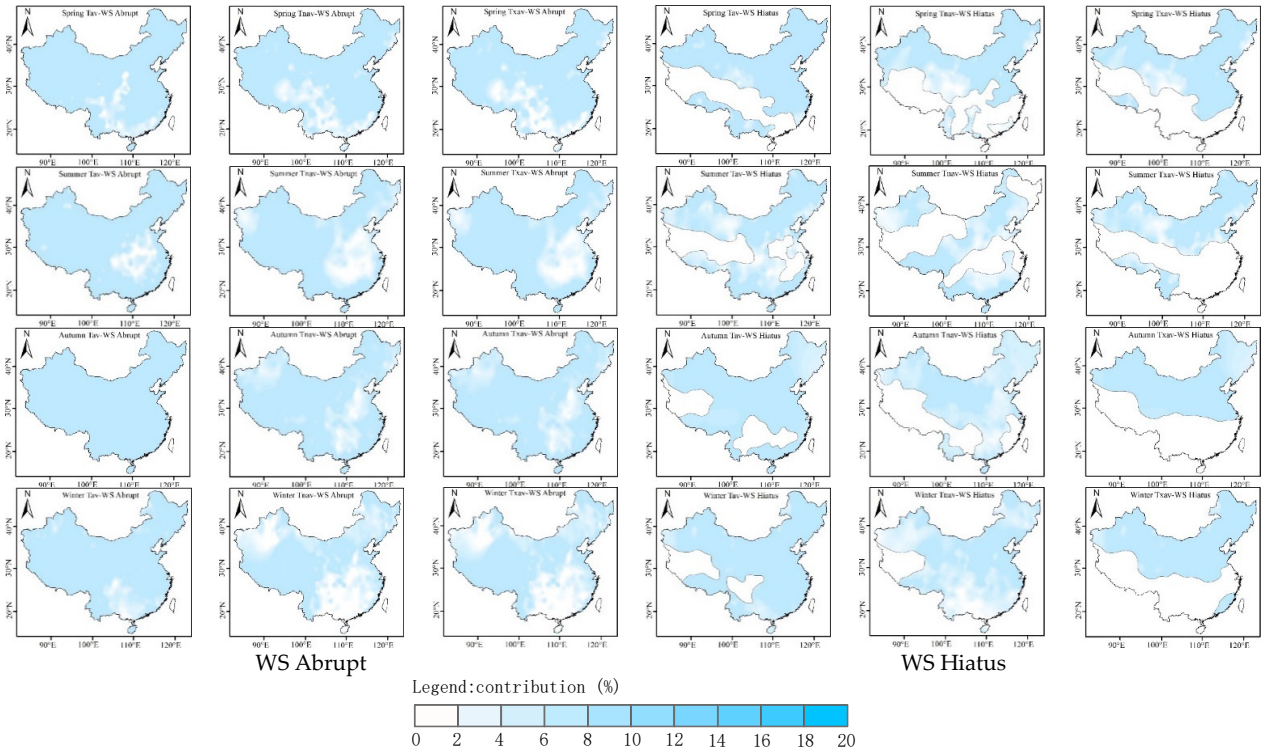

Figure 11. Spatial distributions of the contributions of WS to abrupt changes and warming hiatuses in Tav, Tnav, and Txav.

In the spring, the contributions of WS to warming hiatuses were low in the Tibetan Plateau, the regions south of the Sichuan Basin, and the regions of Guangdong and Guangxi that are characterised by hills, and approximately 6–7% in other regions. In summer, the

contributions of WS to warming hiatuses were high (8–10%) on the central and eastern parts of the Inner Mongolia Plateau. In the autumn, the contributions (approximately 6–7%) of WS to warming hiatuses had a similar spatial distribution but smaller values compared with its contribution to abrupt temperature changes. In the winter, the contributions of WS to warming hiatuses were largest (approximately 8–10%) on the Northeast Plain, the North China Plain, and the eastern part of the Inner Mongolia Plateau.

AP contributed less to abrupt temperature changes than any other regional influencing factor. The contributions of AP to the abrupt temperature change in different seasons followed the descending order of winter > spring > summer > autumn. In the spring, the contributions of AP to abrupt temperature changes were larger (3–6%) in the middle and lower reaches of the Yangtze River, Northeast China, and Northwest China than in other regions. In the summer, the contributions of AP to the abrupt temperature changes were largest (approximately 4%) in the western part of the Yunnan–Guizhou Plateau and approached 0 in Northeast China and the middle and lower reaches of the Yangtze River. In the autumn, the overall contributions of AP to abrupt temperature changes were smallest (<3%) among all seasons. In the winter, the contributions (2–6%) of AP to abrupt temperature changes decreased from north to south.

The contributions of AP to the seasonal warming hiatuses was greater than its contributions to the abrupt temperature changes (Figure 12). In the spring, the contributions of AP to the warming hiatuses were lower in Northeast China and the southern part of the Tibetan Plateau than in other regions (5–7%). In the summer, regions where AP contributed little to warming hiatuses were larger in area than they were in spring, and the contributions of AP to the warming hiatuses were lower in the regions south of the Yangtze River and Northeast China than in other regions (4–6%). In the winter, the contributions of AP to the warming hiatuses (3–7%) were low in the north and high in the south, exhibiting a spatial distribution opposite to that of its contributions to the abrupt temperature changes.

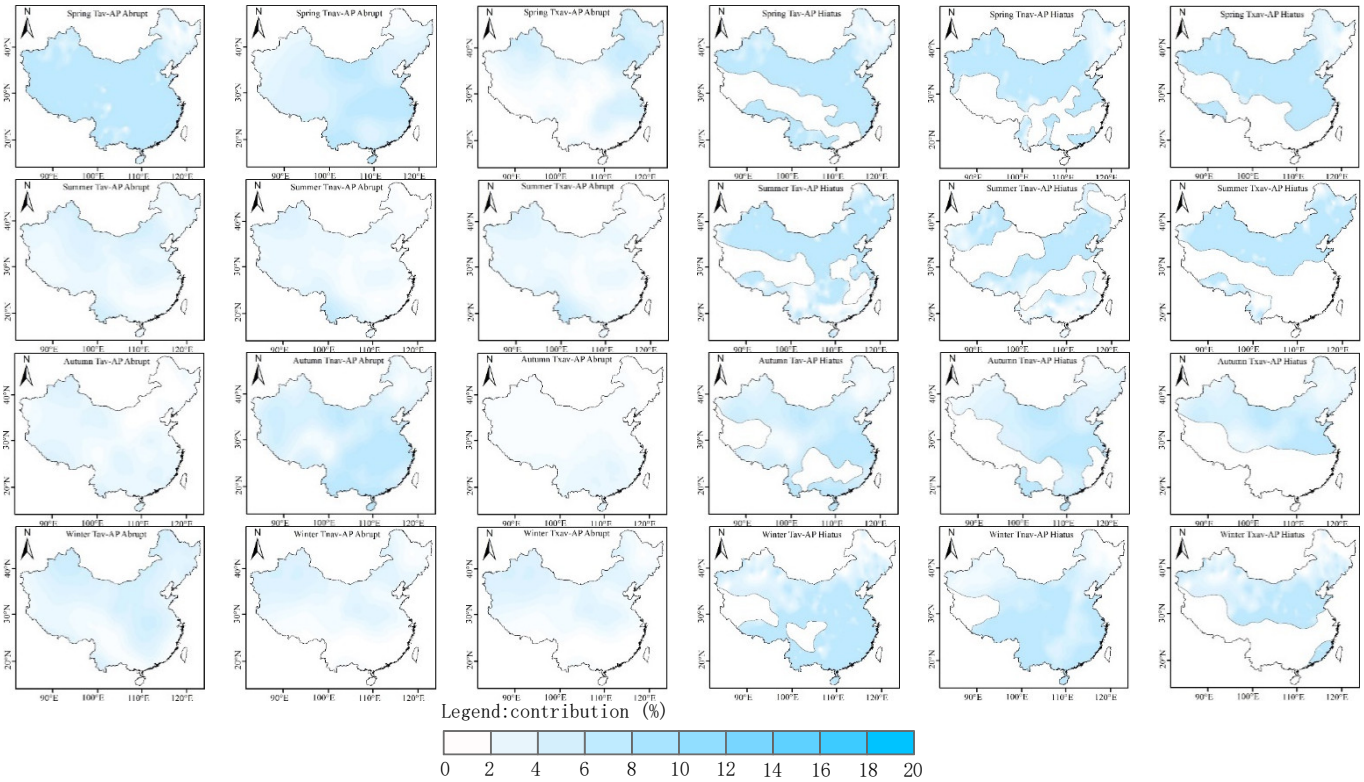

Figure 12. Spatial distributions of the contributions of AP to abrupt changes and warming hiatuses in Tav, Tnav, and Txav.

3.3. The Comprehensive Responses of Seasonal Temperature Abrupt Changes and Warming Hiatuses to Influencing Factors

Taken together, the influencing factors had different degrees of contribution to abrupt seasonal temperature changes and warming hiatuses in China. Figure 13 superimposes the contributions of all influencing factors to abrupt temperature changes. The contributions of the influencing factors to abrupt temperature changes were highest in the spring and summer and lowest in the autumn, demonstrating a large variability between seasons. The PDO, a strong signal of climate variability on the decadal to interdecadal scales, can directly cause interdecadal climate changes over the Pacific Ocean and its surrounding regions (including China) and thus has a great impact on regional and even global climate changes [28]. The contributions of the PDO to abrupt temperature changes had a spatial distribution relatively similar to that of its contributions to warming hiatuses, and both were largest in the winter and smallest in the autumn. However, the PDO contributed more to abrupt temperature changes than to warming hiatuses. In the spring, the PDO made greater contributions (approximately 12%) to the abrupt temperature changes in Northeast China and North China. In the summer, the PDO mainly affected the abrupt temperature changes in regions south of the Yangtze River. In the autumn, the PDO greatly affected Northwest China. The AMO had a large impact on the abrupt temperature changes in most regions of China in all seasons except for in the summer. In the summer, the AMO mainly affected the abrupt temperature changes west of 110° E, with a contribution rate of approximately 11%. The MEI mainly affected the abrupt changes in seasonal temperature in the regions between 25° N and 35° N. When the AO phase is negative, the risk of extremely low-temperature events in northern China rises [29]. In contrast, the persistent enhancement of a positive AO phase leads to the continuous weakening of the East Asia monsoon and the subsequent warming in the norther regions of East Asia in winter [30]. The AO has a great impact on the weather and climate of North America, Europe, and Asia, especially in the winter [31]. The effect of the AO on the mid-latitude surface temperature in the Northern Hemisphere reflects the controlling effect of natural variability on surface temperature. This study also showed that the AO made large contributions (approximately 12%) to the warming hiatuses in winter in Northeast China but low contributions to the abrupt temperature changes and the warming hiatuses in summer. RH had a large impact on the abrupt temperature changes in Southwest China in the spring but a small impact on the abrupt temperature changes in the regions between 25° N and 35° N in the summer. The range of the large RH influence expanded southward and northward in the autumn and covered all regions except for Northwest China in the winter. The contributions of SR to the abrupt changes in Tav, Tnav, and Txav had high spatial variability in all seasons. In the winter, Tav was basically not affected by SR south of the middle and lower reaches of the Yangtze River, while Tnav was less affected by SR overall. The contributions of SR to the abrupt changes in Txav were large (6–7%) on the Northeast and North China Plains. WS had a large impact on the abrupt temperature changes in regions other than the plains of the middle and lower reaches of the Yangtze River. The contribution rates of AP to abrupt temperature changes in the whole country were between 3% and 8%, indicating a small spatial variability.

The range of warming hiatuses had seasonal differences, and the spatial variability of warming hiatuses was relatively little affected by the influencing factors. However, the overall contribution rates of the PDO to seasonal warming hiatuses were high (approximately 12%). The contribution rates of the AO, AMO and MEI to warming hiatuses followed the descending order of AO > AMO > MEI and were smaller than their corresponding contributions to abrupt temperature changes. Among the regional influencing factors, AP and WS strongly affected warming hiatuses, more so than abrupt temperature changes. RH and SR contributed little to warming hiatuses.

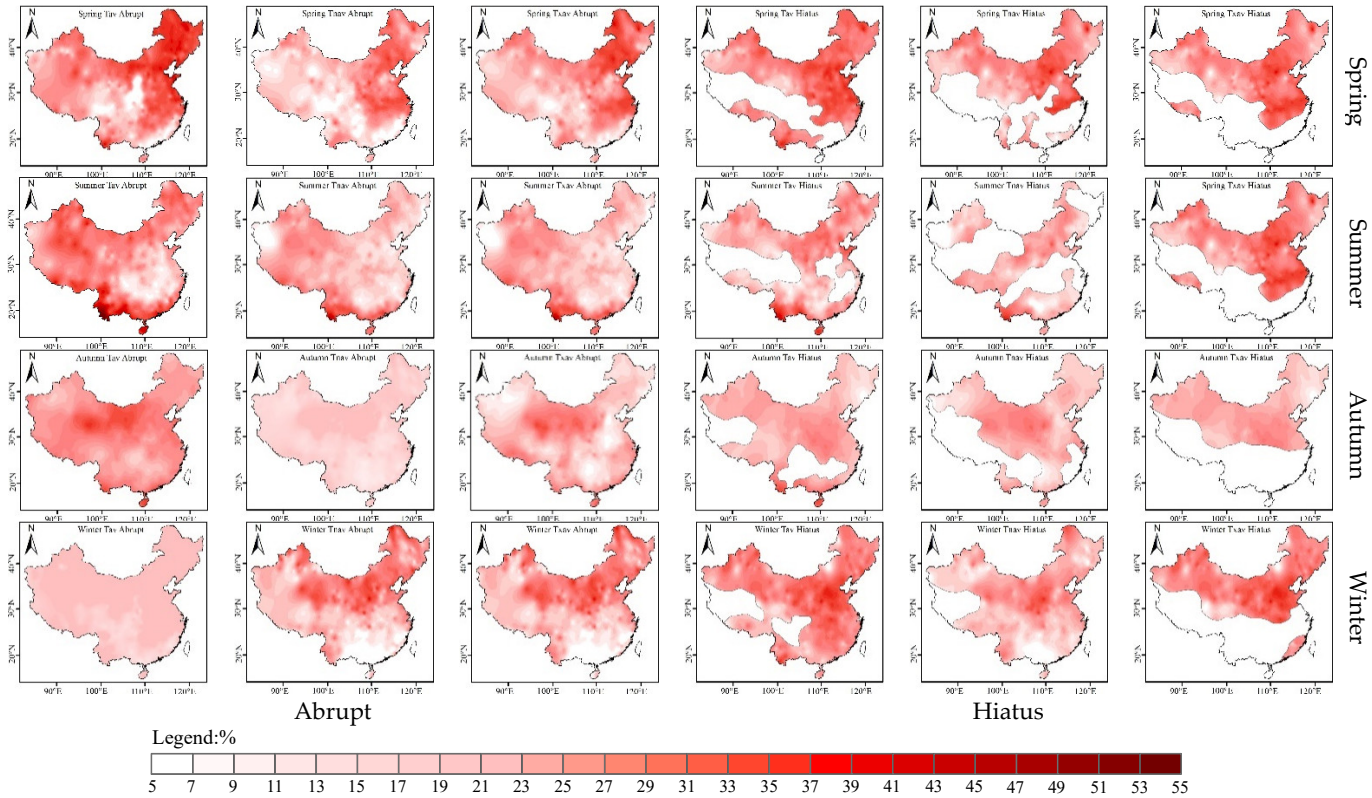

Figure 13. Comprehensive responses of abrupt seasonal changes in Tav, Tnav, and Txav to the influencing factors.

4. Conclusions and Discussion

There are significant differences in the response relationship between the overall change in seasonal temperature and the influencing factors in China. PDO, MEI and AO have the largest and most significant influence on winter temperature; AGG, CO2, RH and AP have the greatest influence on spring temperature; autumn temperature is more sensitive to WS; and summer temperature has the most significant relationship with SR. AGG and CO2 have a significant impact on the abrupt change in air temperature in China, and CO2 contributes significantly to global warming [32]. Although the proportion of CO2 radiative forcing in AGG has decreased, it is not enough to fully explain the phenomenon of temperature warming hiatuses. PDO is consistent with the variation trend of winter temperature in China, which may be an important atmospheric circulation factor affecting the abrupt change in winter temperature [33]. The change in PDO affects the relationship between ENSO and atmospheric circulation, that is, the influence of El Nino and La Nina events on winter temperature in China is not a simple linear relationship [34]. When PDO is in different phases, the relationship between ENSO and the East Asian winter monsoon system is different. When PDO is in the negative phase, the ENSO signals are more likely to propagate to the middle and high latitudes and interact with the East Asian winter monsoon system at middle and high latitudes, thus jointly affecting the winter temperature in China [35]. In addition, the significant warming of China's temperature is related to the warm phase of AMO [36]. Changes in sea surface temperature and sea ice extent contributed about 60% of the Northern Hemisphere summer land warming trend from 1979 to 2008 [37]. Direct warming caused by anthropogenic forcings and indirect warming through rising SST are important reasons for the recent increase in land surface warming and the frequency of hot summers in the Northern Hemisphere [38]. On the whole, as AGG continues to increase, PDO is in a positive phase, AMO and SR continue to rise, MEI mutation, WS, AP and RH continue to decline/rise and the subsequent trend changes, and the temperature changes when the trend rate or value is reached for a certain period of time. In the northern part of

Northwest China, the abrupt temperature change is significantly affected by many factors. On the other hand, the Tibetan Plateau of China was not significantly affected by the factors selected in this study before and after the abrupt temperature change. On the one hand, this may be because the linear relationship between temperature and influencing factors is analysed in this study, while the possible nonlinear relationship between temperature and influencing factors is ignored [39]. On the other hand, the abrupt change in temperature over the Tibetan Plateau in China may be significantly affected by other influencing factors other than those selected in this paper. For example, cloud radiation explains 43 percent of the temperature variation in the southern Tibetan Plateau, The Siberian high [40], the Eurasian Trough [41], and the change in high pressure ridge [42] all significantly affect the temperature change over the Qinghai-Tibet Plateau in China. After abrupt temperature change, some regions of Txav showed a downward trend in each season [43] without cooling stagnation, and most of them concentrated in southern China, which was contrary to the general trend of global warming. According to the results of this analysis, in this region, the decrease in Txav after summer mutation may be significantly affected by SR, because SR is highly consistent with the trend of change before and after summer Txav mutation, However, the decline of spring, autumn and winter seasons after mutation was not significantly affected by the influencing factors, showing that the influencing factors in the warming region after mutation were consistent with the trend of temperature change, while the trend in the cooling region after mutation was inconsistent and weakly correlated. As to why the temperature drops after seasonal mutation, the method of linear relationship study in this paper shows that no specific significant influencing factors and causes can be found from the 10 influencing factors. The first reason may be that the cooling area after Txav mutation is significantly affected by other influencing factors other than the influencing factors selected in this paper. For example, the linear tendency rate of sunshine hours in southern China is negative. Highly consistent with the decreasing trend of air temperature [43], the backscattering of atmospheric aerosols to the lower atmosphere caused by human activities is the main mechanism of the cooling of the lower atmosphere in the Sichuan Basin in southern China [44]. The second possibility is that this study has ignored the potentially significant nonlinear relationship between the temperature change and the influencing factors before and after the abrupt change, which requires us to establish a climate change mechanism model to simulate the nonlinear relationship and further determine the main influencing factors and causes of the temperature drop after the abrupt change.

Author Contributions: X.H. was responsible for the writing, modification and data processing of the paper, L.M. was responsible for the overall idea of the paper, T.L. was responsible for the overall idea of the paper, B.S., Y.C. and Z.Q. were responsible for processing part of the data. All authors have read and agreed to the published version of the manuscript.

Funding: This study was financially supported by the Key technology project of Inner Mongolia Autonomous Region Nos. 2020GG0074. Natural Science Foundation of Inner Mongolia Autonomous Region Nos. 2020MS05054, Inner Mongolia Autonomous Region "Grassland talents" project.

Institutional Review Board Statement: Not applicable.

Informed Consent Statement: Not applicable.

Data Availability Statement: The temperature data used or created in this study can be downloaded from the China National Meteorological Website. http://data.cma.cn/ (accessed on 11 May 2023).

Conflicts of Interest: The authors declare no conflict of interest.

Ethics Approval: All co-authors agree to approve.

References

1. Fu, C.; Diaz, H.F.; Dong, D.; Fletcher, J.O. Changes in atmospheric circulation over northern hemisphere oceans associated with the rapid warming of the 1920s. *Int. J. Climatol.* **2015**, *19*, 581–606. [CrossRef]
2. He, W.P.; Wang, Q.G.; Wu, Q.; Zhang, W.; Zhang, Y. Comparison of characteristics of moving detrended fluctuation analysis with that of approximate entropy method in detecting abrupt dynamic change. *Acta Phys. Sin.* **2009**, *38*, 2862–2871.
3. Wang, Q.G.; Zhang, Z.P. The research of detecting abrupt climate change with approximate entropy. *Acta Phys. Sin.* **2008**, *57*, 1976–1983. [CrossRef]
4. Wang, G.; Zhang, Q.; Luo, M.; Singh, V.P.; Xu, C.-Y. Fractional contribution of global warming and regional urbanization to intensifying regional heatwaves across Eurasia. *Clim. Dyn.* **2022**, *59*, 1521–1537. [CrossRef]
5. Wang, B.; Biasutti, M.; Byrne, M.P.; Castro, C.; Chang, C.P.; Cook, K.; Fu, R.; Grimm, A.M.; Ha, K.-J.; Hendon, H.; et al. Monsoons climate change assessment. *Bull. Amer. Meteor. Soc.* **2021**, *102*, E1–E19. [CrossRef]
6. Kim, Y.H.; Kim, M.K.; Lau, W.K.; Kim, K.M.; Cho, C.H. Possible mechanism of abrupt jump in winter surface air temperature in the late 1980s over the Northern Hemisphere. *J. Geophys. Res. Atmos.* **2015**, *120*, 12474–12485. [CrossRef] [PubMed]
7. Wang, B.; Jin, C.H.; Liu, J. Understanding future change of global monsoons projected by CMIP6 models. *J. Clim.* **2020**, *33*, 6471–6489. [CrossRef]
8. King, M.A.; Bingham, R.J.; Moore, P.; Whitehouse, P.L.; Bentley, M.J.; Milne, G.A. Lower satellite-gravimetry estimates of Antarctic sea-level contribution. *Nature* **2012**, *491*, 586–589. [CrossRef]
9. Qin, W.; Haijun, Y. Investigating the role of the Tibetan Plateau in the formation of Pacific meridional overturning circulation. *J. Clim.* **2020**, *33*, 3603–3617.
10. Xiao, D.; Li, J.P. Spatial and temporal characteristics of the decadal abrupt changes of atmosphere-ocean system in 1970s. *J. Geophys. Res.* **2007**, *112*, D24S22. [CrossRef]
11. Zhang, Q.; Wu, Z.; Yu, H.; Zhu, X.; Shen, Z. Variable urbanization warming effects across metropolitans of China and relevant driving factors. *Remote Sens.* **2020**, *12*, 1500. [CrossRef]
12. Zhenyu, H.; Bo, W.; Xiaoge, X. Decadal prediction skill of the global sea surface temperature in the BCC-CSM1.1 climate model. *Adv. Earth Sci.* **2017**, *32*, 396–408. [CrossRef]
13. Delworth, T.L.; Zeng, F.; Rosati, A.; Vecchi, G.A.; Wittenberg, A.T. A link between the Hiatus in global warming and North American drought. *J. Clim.* **2015**, *28*, 3834–3845. [CrossRef]
14. Ueda, H.; Kamae, Y.; Hayasaki, M.; Kitoh, A.; Watanabe, S.; Miki, Y.; Kumai, A. Combined effects of recent Pacific cooling and Indian Ocean warming on the Asian monsoon. *Nat. Commun.* **2015**, *6*, 8854. [CrossRef]
15. Jiuwei, Z.; Ruifen, Z.; Yuqing, W. Global warming hiatus contributed to the increased occurrence of intense tropical cyclones in the coastal regions along East Asia. *Sci. Rep.* **2018**, *8*, 6023. [CrossRef]
16. Johnson, N.C.; Xie, S.P.; Kosaka, Y.; Li, X. Increasing occurrence of cold and warm extremes during the recent global warming slowdown. *Nat. Commun.* **2018**, *9*, 1724. [CrossRef]
17. Wang, X.; Xiao, J.; Li, X.; Cheng, G.; Ma, M.; Zhu, G.; Arain, M.A.; Black, T.A.; Jassal, R.S. No trends in spring and autumn phenology during the global warming hiatus. *Nat. Commun.* **2019**, *10*, 2389. [CrossRef]
18. Huang, J.; Xie, Y.; Guan, X.; Li, D.; Ji, F. The dynamics of the warming hiatus over the Northern Hemisphere. *Clim. Dyn.* **2017**, *48*, 429–446. [CrossRef]
19. Sun, S.; Zhang, Q.; Singh, V.P.; Shi, C.; Wang, G.; Wu, W.; Shen, Z. Increased moist heat stress risk across China under warming climate. *Sci. Rep.* **2022**, *12*, 22548. [CrossRef]
20. Xing, Z.; Tianjun, Z.; Wenxia, Z.; Lixia, Z. Global Monsoon Simulated by FGOALS-g3 Climate System Model: A Comparison with the Previous Version and Influences of Air–Sea Coupling. *Chin. J. Atmos. Sci.* **2003**, *47*, 470–486. (In Chinese) [CrossRef]
21. Karl, T.R.; Arguez, A.; Huang, B.; Lawrimore, J.H.; McMahon, J.R.; Menne, M.J.; Peterson, T.C.; Vose, R.S.; Zhang, H. Possible artifacts of data biases in the recent global surface warming hiatus. *Science* **2015**, *348*, 1469–1472. [CrossRef]
22. Xiang, L.Y.; Chen, X. Regional and Seasonal Features of Abrupt Temperature Change in China in Recent 55 Years. *Meteorological* **2006**, *32*, 44–47.
23. Wang, H.; Chen, Y.; Xun, S.; Lai, D.; Fan, Y.; Li, Z. Changes in daily climate extremes in the arid area of northwestern China. *Theor. Appl. Climatol.* **2013**, *112*, 15–28. [CrossRef]
24. Zhang, X.L.; Hua, L.J.; Jiang, D.B. Assessment of CMIP6 model performance for temperature and precipitation in Xinjiang, China. *Atmos. Oceanic Sci. Lett.* **2022**, *15*, 100128. [CrossRef]
25. Fyfe, J.C.; Meehl, G.A.; England, M.H.; Mann, M.E.; Santer, B.D.; Flato, G.M.; Hawkins, E.; Gillett, N.P.; Xie, S.P.; Kosaka, Y. Making sense of the early-2000s warming slow-down. *Nat. Clim. Chang.* **2016**, *6*, 224–228. [CrossRef]
26. Dai, A.; Fyfe, J.C.; Xie, S.P.; Dai, X. Decadal modulation of global surface temperature by internal climate variability. *Nat. Clim. Chang.* **2015**, *5*, 555–559. [CrossRef]
27. Nan, S.; Li, J. The relationship between the summer precipitation in the Yangtze River valley and the boreal spring Southern Hemisphere annular mode. *Geophys. Res. Lett.* **2003**, *30*, 2266. [CrossRef]
28. Meehl, G.A.; Hu, A.; Santer, B.D.; Xie, S.P. Contribution of the Interdecadal Pacific Oscillation twenieth-century global surface temperature trends. *Nat. Clim. Chang.* **2016**, *6*, 1005–1008. [CrossRef]
29. Zuo, J.Q. Relationship between AO/NAO and ENSO and Their Impact on Climate Anomalies in China. Ph.D. Thesis, Lanzhou University, Lanzhou, China, 2011.

30. Li, L.; Yu, Y.; Tang, Y.; Lin, P.; Xie, J.; Song, M.; Dong, L.; Liu, L.; Wang, L.; Pu, Y.; et al. The flexible global ocean–atmosphere–land system model grid-point version 3 (FGOALS-g3): Description and evaluation. *J. Adv. Model. Earth Syst.* **2020**, *12*, e2019MS002012. [CrossRef]
31. Thompson, D.W.; Lee, S.; Baldwin, M.P. Atmospheric processes governing the northern hemisphere annular mode/North Atlantic oscillation. *North Atl. Oscil. Clim. Significance Environ. Impact* **2003**, *134*, 81–112. [CrossRef]
32. Fan, Y.; Ying, C. Research progress summarization for the impacts of global climate change to the regional water resoueces. *J. Water Resour. Water Eng.* **2008**, *19*, 92–97+102.
33. Wang, D.; Sun, Y.C.; You, Q.L. Contribution of Pacific Decadal Oscillation to interdecadal variability of winter minimum temperature in China. *Clim. Chang. Res.* **2020**, *16*, 70–77.
34. Ding, R.; Ha, K.; Li, J. Interdecadal shift in the relationship between the East Asian summer monsoon and the tropical Indian Ocean. *Clim. Dyn.* **2010**, *34*, 1059–1071. [CrossRef]
35. Wang, L.; Chen, W.; Huang, R.H. Interdecadal modulation of PDO on the impact of ENSO on the East Asian winter monsoon. *Geophys. Res. Lett.* **2008**, *35*, L20702. [CrossRef]
36. Junhui, Y.; Quansheng, G.; Jingyun, Z. Reconstruction and Analysis on the Series of Winter-half-year Temperature Change during the Qing Dyn asty in the Northern China Region. *Prog. Geogr.* **2012**, *31*, 1426–1432.
37. Andrews, T. Using an AGCM to diagnose historical effective radiative forcing and mechanisms of recent decadal climate change. *J. Climate* **2014**, *27*, 1193–1209. [CrossRef]
38. Kamae, Y.; Shiogama, H.; Watanabe, M.; Kimoto, M. Attributing the increase in Northern Hemisphere hot summers since the late 20th century. *Geophys. Res. Lett.* **2014**, *41*, 5192–5199. [CrossRef]
39. Chen, L.; Zhu, W.; Zhou, X.; Zhu, W.Q. Variation of atmospheric aerosol depth in China during recent 52 years. *J. Geo. Phy. Res.* **2004**, *27*, 634–646.
40. Wu, B.Y.; Su, J.Z.; Zhang, R.H. Effects of autumn-winter Arctic sea ice on winter Siberian High. *Chin. Sci. Bull.* **2011**, *56*, 3220–3228. [CrossRef]
41. Gao, Y.; Cuo, L.; Zhang, Y. Changes in moisture flux over the Tibetan Plateau during 1979–2011 and possible mechanisms. *J. Clim.* **2014**, *27*, 1876–1893. [CrossRef]
42. Pepin, N.; Bradley, R.S.; Diaz, H.F.; Baraër, M.; Caceres, E.B.; Forsythe, N.; Fowler, H.; Greenwood, G.; Hashmi, M.Z.; Liu, X.D.; et al. Elevation-dependent warming in mountain regions of the world. *Nat. Clim. Chang.* **2015**, *5*, 424–430.
43. Yunfeng, L.; Weiliang, L.; Xiuji, Z.; Qing, H.; Jizu, Q. Analysis of the atmospheric aerosol optical depth over China in 1980s. *Acta Meteor Sin.* **2000**, *14*, 490–502.
44. Huang, X.; Ma, L.; Liu, T.; Sun, B.; Zhou, Y.; Yang, C.; Qiao, Z. Spatial and temporal variability of the abrupt interannual temperature change and warming hiatus in China, 1951–2016. *Meteorol. Appl.* **2020**, *27*, e1911. [CrossRef]